

# Surface ocean density gradients during the Last Glacial Maximum

K. Billups and D. P. Schrag

Laboratory for Geochemical Oceanography, Department of Earth and Planetary Sciences, Harvard University, Cambridge, Massachusetts

**Abstract.** We have compiled published planktonic foraminiferal oxygen isotope values from the tropical to subtropical Atlantic and Pacific for the late Holocene and Last Glacial Maximum (LGM). We interpret the spatial distribution of  $\delta^{18}\text{O}$  values in terms of meridional density gradients in the LGM surface ocean and discuss implications on tropical ocean thermocline structure. In both oceans, glacial  $\delta^{18}\text{O}$  values display a pattern of interhemispheric asymmetry evidenced by increasingly higher glacial  $\delta^{18}\text{O}$  values toward northern latitudes. The  $\delta^{18}\text{O}$ -derived density estimates suggest that the northern subtropical surface ocean density was higher during the LGM than today, which has significant implications on LGM thermocline ventilation. In the Atlantic, steeper density gradients in the northern subtropics during the LGM are consistent with a more compressed subtropical gyre and thermocline water formation farther south than today. In the Pacific the steeper density gradients suggest a significant reduction in freshwater fluxes to the northern tropical and subtropical regions, which raises the possibility of a more significant component of Northern Hemisphere source waters to the tropical Pacific thermocline. These predictions could be tested with numerical ocean models that assess the structure of the tropical thermocline in the glacial ocean.

## 1. Introduction

In this study we make use of existing planktonic foraminiferal  $\delta^{18}\text{O}$  data from the tropical and subtropical surface Atlantic and Pacific (Figure 1 and Table 1<sup>1</sup>) and explore their utility as a tracer for surface water density. This density approach is important because it circumvents the need to dissect the foraminiferal  $\delta^{18}\text{O}$  values into temperature and salinity components for meaningful paleoceanographic reconstructions. Temperature and salinity define the density of sea water, a property that by itself has significant implications for ocean dynamics regardless of the individual temperature/salinity constituent. While we forgo quantification of past sea surface temperatures (SST), we do not wish to relinquish entirely a discussion of temperature versus salinity changes in accordance with previous studies. However, our primary goal is to demonstrate that planktonic foraminiferal  $\delta^{18}\text{O}$  values can be used to reconstruct meridional surface water density gradients. We focus our discussion on implications on glacial age tropical thermocline structure.

### 1.1. Background

Planktonic foraminiferal  $\delta^{18}\text{O}$  data are commonly used to reconstruct SST [e.g., Broecker, 1986; Sikes and Keigwin, 1994; Billups and Spero, 1996; Stott and Tang, 1996; Curry

and Oppo, 1997; Wolff *et al.*, 1998]. The accuracy of the magnitude of glacial to interglacial temperature variability derived from a foraminiferal  $\delta^{18}\text{O}$  time series, however, hinges on the validity of assumptions about glacial to interglacial changes in the isotopic composition of the whole ocean reservoir as well as the ambient sea water. Between the Last Glacial Maximum (LGM) and the late Holocene (LH) the whole ocean reservoir reflects an  $^{18}\text{O}$  depletion due to the decay of continental ice sheets. The corresponding shift in the  $\delta^{18}\text{O}$  values of sea water was estimated by Schrag *et al.* [1996] to be 1‰ on average. Unfortunately, as of yet, there is no independent measure for past changes in local evaporation versus precipitation (*E-P*) patterns, which determine the local surface water salinity and ambient sea water oxygen isotopic composition ( $\delta^{18}\text{O}_w$ ). A numerical exercise by Norton *et al.* [1997] portrays the sensitivity of LH to LGM temperature reconstructions to assumptions of glacial surface ocean *E-P* and associated  $\delta^{18}\text{O}_w$ .

Salinity and temperature effects that convolute a foraminiferal  $\delta^{18}\text{O}$  signal also define the density of sea water in which a shell calcifies, and a relationship exists between the two parameters [Lynch-Stieglitz *et al.*, 1999]. Lynch-Stieglitz *et al.* [1999] discuss the application of benthic foraminiferal  $\delta^{18}\text{O}$  values to tracing upper ocean density and geostrophic transport. Eshel *et al.* [1999] demonstrate that Red Sea coral  $\delta^{18}\text{O}$  values are highly correlated with local sea water density, an observation that allowed the reconstruction of vertical water mass stability. In the tropical to subtropical surface oceans,  $\delta^{18}\text{O}$  values of predicted calcite ( $\delta^{18}\text{O}_c$ ) (calculated from  $\delta^{18}\text{O}_w$  values and SST) also correlate well with surface water density ( $r=0.98$ ) (Figure 2). Thus we show that planktonic foraminiferal  $\delta^{18}\text{O}$  values can also be used as a proxy for surface water density, at least at temperatures and salinities characterizing the tropical to subtropical surface ocean (15–28°C and 33–36, respectively).

<sup>1</sup>Supporting data are available electronically at World Data Center-A for Paleoclimatology, NOAA/NGDC, 325 Broadway, Boulder, Colorado (e-mail: paleo@mail.ngdc.noaa.gov; URL: <http://ngdc.noaa.gov/paleo>).

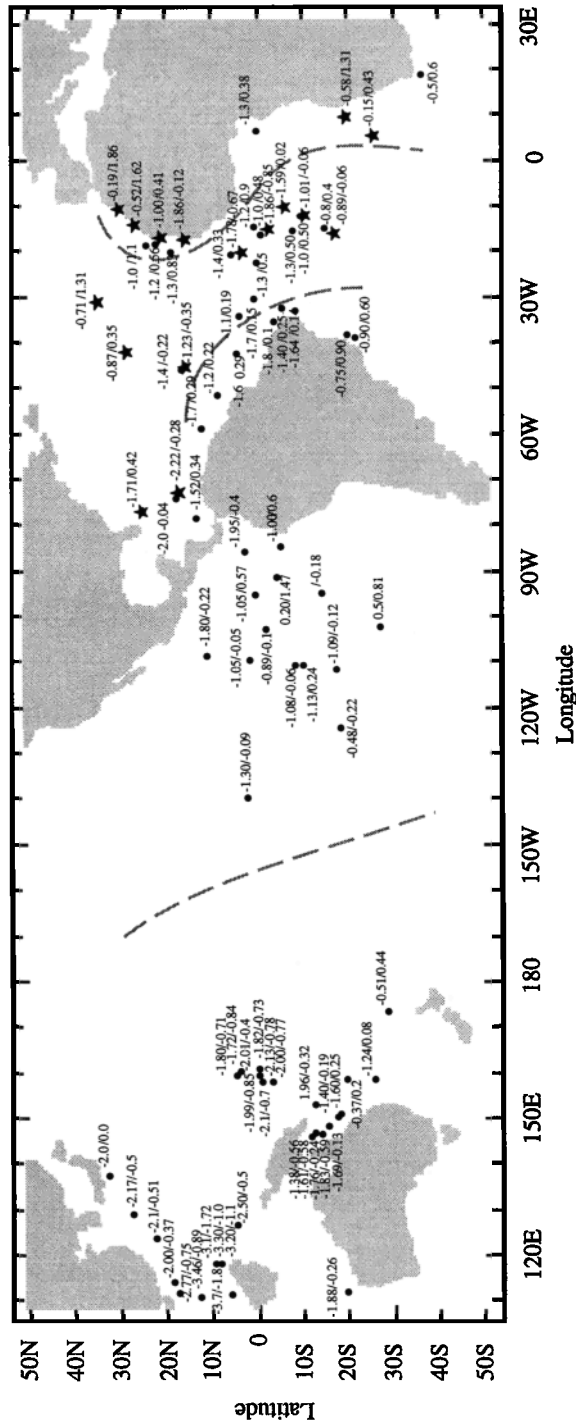


Figure 1. Compilation of Atlantic and Pacific planktonic foraminiferal oxygen isotope data from the late Holocene and Last Glacial Maximum. Circles indicate data from *Globigerinoides sacculifer* and stars designate data from *Globigerinoides ruber* (white). Each ocean was subdivided into a western, central (Atlantic only), and eastern region (dashed lines).

## 1.2. Modern Ocean Density and $\delta^{18}\text{O}$ Gradients

Meridional surface water temperature and salinity gradients determine the meridional gradients in density and  $\delta^{18}\text{O}_c$  (Figure 3). Temperature has a maximum at the equator, reflecting maximum energy input into the ocean by the Sun, which diminishes poleward. Salinity is relatively low just north of the equator because of excess precipitation associated with atmospheric updrafts in the region of trade wind convergence and relatively high at  $\sim 25^\circ\text{N}$  and  $\sim 25^\circ\text{S}$  because of excess evaporation underneath the trade wind belts. The salinity and  $^{18}\text{O}/^{16}\text{O}$  ratio (not shown) of sea water are linearly related on the regional scale by evaporation and vapor transport processes [Fairbanks *et al.*, 1992; Craig and Gordon, 1965]. Density varies predominantly as a function of temperature in the open ocean [e.g., Pickard and Emery, 1990; Pond and Pickard, 1983], hence its meridional profile largely follows the meridional temperature gradient (Figure 3). Increasing calcite  $\delta^{18}\text{O}$  values with latitude reflects chiefly the decrease in ambient surface water temperatures (Figure 3); the reconstruction of absolute SST, however, would rely on knowledge of the local isotopic composition of sea water.

Wind and wind-driven surface currents redistribute surface water masses in the upper ocean and determine local gradients in temperature, salinity (and hence the  $\delta^{18}\text{O}$  of surface water and biogenic calcite), and density. For example, easterly wind stress in tropical to subtropical regions leaves the Atlantic surface ocean relatively enriched and the Pacific sea surface relatively depleted in salt (and  $^{18}\text{O}$ ). Relatively large zonal gradients exist in temperature and salinity in the tropical and subtropical oceans within ocean basins because of the predominantly easterly wind stress driving cooler subsurface water to the sea surface in the equatorial regions, along eastern boundaries, and then "piling up" radiatively heated water along the western margins. In the western tropical Pacific, easterly wind stress also leads to important ocean-atmosphere interactions (e.g., the Walker Circulation) which can significantly alter average climate conditions [e.g., Peixoto and Oort, 1992]. Here SST can exceed  $30^\circ\text{C}$ , and intense atmospheric updrafts and associated heavy rainfall keep the sea surface relatively fresh (33-34) and of low density ( $1022 \text{ kg m}^{-3}$ ) [Levitus and Boyer, 1994]. To avoid averaging data over such differing hydrographic regimes, we have grouped each ocean basin into a western, central (Atlantic only), and eastern region. Within each region, the data can then be evaluated in a series of south-to-north transects (Figures 4-7) and yield a spatially resolved picture of glacial to interglacial changes in surface ocean density gradients.

## 2. Methods

In this study we have compiled LH and LGM *Globigerinoides sacculifer* (with and without a sac-like final chamber) and *Globigerinoides ruber* (white)  $\delta^{18}\text{O}$  data from the Atlantic and Pacific (Figure 1 and Table 1). *G. sacculifer* and *G. ruber* are two planktonic species that calcify within the surface mixed layer. *G. ruber* predominantly calcifies in the surface most regions of the mixed layer, while *G. sacculifer* has a more expanded depth

Table 1. Late Holocene (LH) and Last Glacial Maximum (LGM) Planktonic Foraminiferal  $\delta^{18}\text{O}$  values

Species and Core	Latitude, °N	Longitude, °E	Depth, m	Sedimentation Rates, $\frac{\text{cm}}{\text{kyr}}$	LH $\delta^{18}\text{O}$ , ‰	LGM $\delta^{18}\text{O}$ , ‰	$\Delta\delta^{18}\text{O}$ , ‰	Reference
<i>Western Atlantic</i>								
<i>G. sacculifer</i>								
GeoB 3202-1	-21.6	-40	1090	4.5	-0.90	0.60	1.50	1
GeoB 3229-2	-19.6	-38.75	780	4.5	-0.75	0.90	1.65	1
Mean -22° to -20°N	-20.6				-0.83	0.75	1.58	
GeoB 3176-1	-7	-34.5	1385	17	-1.40	0.25	1.65	1
GeoB 2204	-8.5	-34.0	2072	2	-1.64	0.14	1.78	2
GeoB 3129-1	-4.5	-36.6	830	38	-1.50	0.30	1.80	1
GeoB 3117-1	-4.2	-37.1	930	14	-1.50	0.50	2.00	1
GeoB 3104-1	-3.6	-37.6	767	6	-1.30	0.40	1.70	1
V25-56	-3.6	-35.2	3512	4	-1.82	0.10	1.92	3
Mean -9° to -4°N	-5.2				-1.53	0.28	1.81	
GeoB 1523-1	3.8	-41.6	3292	2	-1.87	0.24	2.11	2
RC13-184	3.9	-43.3	3446	4	-1.43	0.13	1.56	3
KNR 110-82GGC	4.3	-43.5	2816	3	-1.61	0.39	2.00	4
KNR110-43PC	4.7	-43.7	3436	3	-1.61	0.24	1.85	4
V25-75	8.6	-53.2	2743	8	-1.24	0.22	1.46	3
Mean 4°-9°N	5.1				-1.55	0.24	1.80	
RC9-49	11.2	-58.6	1851	4	-1.70	0.29	1.99	3
V28-122	11.9	-78.7	3623	7	-1.53	0.35	1.87	5
A179-4	16.6	-74.8	2963	2	-1.80	0.00	1.80	6
V12-122	17.0	-74.4	2800	2	-2.19	-0.07	2.12	7
Mean 11°-17°N	14.2				-1.80	0.14	1.95	
<i>G. ruber (white)</i>								
V12-122	17.0	-74.4	2800	3	-2.39	-0.30	2.09	7
A179-4	16.6	-74.8	2963	2	-2.04	-0.26	1.78	8
Mean 17°N	16.8				-2.22	-0.28	1.94	
OC205-2-108GGC	26.0	-78.2	730	8	-1.97	0.62	2.59	9
OC205-2-103GGC	26.1	-78.1	950	9	-1.78	0.82	2.60	9
OC205-2-100GGC	26.1	-78.0	1045	8	-1.68	0.44	2.12	9
OC205-2-97JPC	25.9	-77.9	1172	3	-1.54	0.55	2.09	9
OC205-2-33GGC	26.2	-77.7	770	5	-1.57	0.33	1.90	9
OC205-2-149JPC	26.3	-77.7	423	13	-1.55	0.32	1.87	9
CH01-82 42PC	26.2	-77.6	985	6	-1.81	0.03	1.84	9
CH01-82-36PC	26.2	-77.6	651	3	-1.74	0.17	1.91	9
Mean 26°N	26.1				-1.71	0.41	2.12	

Table 1. (continued)

Species and Core	Latitude, °N	Longitude, °E	Depth, m	Sedimentation Rates cm kyr <sup>-1</sup>	LH $\delta^{18}\text{O}$ , ‰	LGM $\delta^{18}\text{O}$ , ‰	$\Delta\delta^{18}\text{O}$ , ‰	Reference
<i>Central Atlantic</i>								
<i>G. sacculifer</i>								
INMD 115	-17.6	-16.2	3427	1	-0.66	0.39	1.05	10
INMD 111	-12.7	-13.9	3069	2	-0.98	0.41	1.39	10
V22-174	-10.1	-12.8	2630	3	-0.90	0.70	1.60	11
INMD 110	-10.0	-13.4	1959	2	-1.06	0.27	1.32	10
V22-177	-7.8	-14.6	3290	3	-1.31	0.50	1.81	3
Mean -18° to -8°N	-10.1				-1.06	0.47	1.53	
V22-182	-0.6	-17.3	3776	4	-0.97	0.48	1.45	3
V30-40	-0.2	-23.2	3706	4	-1.30	0.50	1.80	12
A180-73	0.2	-23.0	3.7	3	-1.40	0.40	1.80	6
246	0.8	-31.5	3200	4	-1.70	0.00	1.70	6
RC13-189	1.9	-30.0	3233	3	-1.73	0.30	2.03	3
16771-2	0.8	-15.5	2764	3	-1.15	0.90	2.05	13
Mean -1°-2°N	0.5				-1.38	0.43	1.81	
V25-60	3.3	-34.8	3749	2	-1.08	0.19	1.27	3
INMD 104	4.3	-21.9	3279	2	-1.10	0.19	1.29	10
13519-1	5.7	-19.9	2862	2	-1.35	0.45	1.80	13
234	5.8	-21.7	3600	3	-1.70	0.00	1.70	6
Mean 3°-6°N	4.7				-1.31	0.21	1.52	
INMD 97	16.7	-46.1	3619	2	-1.38	-0.22	1.17	10
<i>G. ruber</i> (white)								
INMD 115	-17.6	-16.2	3427	1	-0.89	-0.06	0.83	10
INMD 111	-12.7	-13.9	3069	2	-1.06	-0.06	1.00	10
INMD 110	-10.0	-13.4	1959	2	-0.96	-0.07	0.89	10
Mean -13° to -10°N	-11.3				-1.01	-0.06	0.95	
GeoB1113-47	-5.7	-11.0	2374	4	-1.59	0.20	1.79	10
INMD 108	-2.0	-16.0	3895	1	-1.86	-0.85	1.01	10
INMD 104	4.3	-21.9	3279	2	-1.78	-0.67	1.11	10
Mean -6°-4°N	-1.2				-1.74	-0.44	1.30	
INMD 97	16.7	-46.1	3619	2	-1.23	-0.35	0.88	10
V22-222	28.9	-43.7	3197	3	-0.87	0.35	1.22	3
V32-08	34.8	-32.4	3252	4	-0.71	1.31	2.02	3

Table 1. (continued)

Species and Core	Latitude, °N	Longitude, °E	Depth, m	Sedimentation Rates cm kyr <sup>-1</sup>	LH δ <sup>18</sup> O, ‰	LGM δ <sup>18</sup> O, ‰	Δδ <sup>18</sup> O, ‰	Reference
<i>Eastern Atlantic</i>								
<i>G. sacculifer</i>								
RC11-86	-35.8	18.4	2800	7	-0.50	0.60	1.10	6
V29-144	-0.2	6.1	2685	4	-1.26	0.38	1.64	3
13289-1/2	18.1	-18.9	2470	3	-1.50	0.80	2.30	13
V30-49	18.4	-21.1	3093	4	-1.26	0.38	1.64	3
12329-4/6	19.4	-19.9	3314	3	-1.20	0.95	2.15	13
16030-1	21.2	-18.1	1500	5	-1.15	0.56	1.71	13
Mean 18°-21°N	19.3				-1.28	0.67	1.95	
12310-3/4	23.5	-18.7	3076	6	-1.00	1.10	2.10	13
<i>G. ruber</i> (white)								
V19-248	-24.5	4.8	3321		-0.15	0.43	0.58	14
GeoB1028-5	-20.1	9.2	2209	5	-0.58	1.31	1.89	15
Mean -25° to -20°N	-22.3				-0.37	0.87	1.24	
12337-5 KC	16.0	-18.1	3094	7	-1.86	-0.12	1.74	13
16017-2	21.3	-17.8	812	13	-1.00	0.41	1.41	13
M12309	26.8	-15.1	2849	6	-0.52	1.62	2.14	13
Mean 16° to -27°N	21.3				-1.13	0.64	1.76	
16004-1	30.0	-10.6	1512	4	-0.19	1.86	2.05	13
<i>Western Pacific</i>								
<i>G. sacculifer</i>								
RC9-124	-28.7	172.59	2540	1	-0.51	0.44	0.95	14
RC12-109	-25.9	157.87	2930	2	-1.24	0.08	1.32	16
RC12-113	-25.0	163.50	2454	2	-0.37	0.2	0.57	16
Mean -29° to -25°N	-26.5				-0.71	0.24	0.95	
ODP 817A	-19.2	149.76	1016	7	-1.60	0.25	1.85	17
RC11-147	-19.1	112.80	2000	3	-1.88	-0.26	1.62	14
V24-161	-18.2	151.45	1670	2	-1.40	-0.19	1.21	16
ODP 818B	-18.1	150.04	745	10	-1.69	-0.13	1.56	17
Mean -19° to -18°N	-18.6				-1.64	-0.08	1.56	
ODP 821	-16.6	146.29	212	6	-1.83	-0.59	1.24	18
V24-157	-16.0	147.92	1212	2	-1.76	-0.24	1.52	16
RC10-131	-14.5	157.97	2933	3	-1.96	-0.32	1.64	16
V24-170	-13.5	146.88	2243	2	-1.61	-0.58	1.03	16
V24-184	-13.0	146.20	2992	1	-1.38	-0.56	0.82	16
Mean -17° to 13°N	-14.7				-1.71	-0.46	1.25	

Table 1. (continued)

Species and Core	Latitude, °N	Longitude, °E	Depth, m	Sedimentation Rates cm kyr <sup>-1</sup>	LH δ <sup>18</sup> O, ‰	LGM δ <sup>18</sup> O, ‰	Δδ <sup>18</sup> O, ‰	Reference
ERDC 93P	-2.2	157.01	1619	1	-2.13	-0.78	1.35	19
ERDC92	-2.2	157.00	1598	2	-2.00	-0.765	1.24	20
MW91-15	0.0	159.00	2311	3	-2.10	-0.7	1.40	21
ERDC128	0.0	161.40	3700	2	-1.82	-0.73	1.09	20
ODP 806B	0.0	159.50	2600	16	-1.98	-0.85	1.13	22
V24-109	0.4	158.80	2367	2	-2.01	-0.4	1.61	19
V28-238	1.0	160.80	3120	2	-1.90	-0.96	0.94	14
ERDC 84P/PG	1.4	157.26	2339	2	-1.80	-0.8	1.00	23
RC17-177	1.8	159.45	2600	2	-2.04	-0.64	1.40	19
V28-239	3.3	159.18	3490	1	-1.72	-0.84	0.88	14
V28-235	5.5	160.50	1700	2	-1.80	-0.71	1.09	14
WP-2	6.3	126.43	1580	4	-2.50	-0.5	2.00	24
GGC 23	8.2	118.57	990	7	-3.30	-1	2.30	25
GGC 27	8.5	118.25	2030	4	-3.20	-1.1	2.10	25
Mean -2°-9°N	2.3				-2.16	-0.77	1.39	
GGC 13	10.6	118.29	990	4	-3.10	-1.72	1.38	26
GGC 9	11.6	118.62	1465	6	-3.70	-1.8	1.90	25
GGC 10	11.7	118.51	1605	6	-3.34	-1.63	1.71	26
GGC 11	11.9	118.33	2165	4	-2.94	-1.41	1.53	26
GGC 12	11.9	112.21	2495	4	-3.46	-0.89	2.57	26
GGC 6	12.2	118.07	2975	3	-3.28	-1.4	1.88	26
GGC 4	12.7	117.93	3530	5	-3.07	-1.05	2.02	26
WP-1	13.8	125.57	2208	3	-2.50	-0.8	1.70	24
Mean 11°-14°N	12.0				-3.17	-1.34	1.84	
SO50 29KL	18.4	115.65	3766	5	-1.90	-0.07	1.83	27
V36-06-3	19.0	116.09	2809	≥10	-2.00	-0.37	1.63	28
SO49-KL8	19.2	114.20	1040	5	-2.77	-0.75	2.02	28
V28-255	20.0	142.50	3261	1	-0.9	-0.9	1.59	14
WP-3	22.2	122.95	2700	3	-2.10	-0.51	1.59	24
Mean 18°-22°N	19.2				-2.22	-0.52	1.83	
Z14-6	27.1	127.45	739	4	-2.17	-0.5	1.67	24
C-4	33.2	137.70	3342	7	-2.00	0	2.00	29
Mean 27°-33°N	30.1				-2.09	-0.25	1.84	
<i>Eastern Pacific</i>								
<i>G. sacculifer</i>								
RC8-94	-27.28	-102.08	3074	1	0.05	0.81	0.76	14
RC13-81	-19.02	-124.22	3751	2	-0.48	-0.22	0.26	14
V19-55	-17.00	-114.18	3177	1	-1.09	-0.12	0.97	14

Table 1. (continued)

Species and Core	Latitude, °N	Longitude, °E	Depth, m	Sedimentation Rates cm kyr <sup>-1</sup>	LH $\delta^{18}\text{O}_c$ , ‰	LGM $\delta^{18}\text{O}_c$ , ‰	$\Delta\delta^{18}\text{O}_c$ , ‰	Reference
Mean -27° to -17°N	-18.01				-0.79	-0.17	0.62	
V19-41	-14.10	-96.20	3248			-0.18		14
Y71-7-45P	-11.00	-111.00	3096	1	-1.13	0.24	1.37	14
RC11-230	-8.80	-110.80	3300	2	-1.08	-0.06	1.02	14
Mean -14° to -9°N	-11.30				-1.11	0.00	1.20	
TR163-31B	-4.00	-84.00	2311	10	-1.00	0.6	1.60	21
V21-33	-3.80	-92.10	3700	2	0.20	1.47	1.27	14
RC13-113	-1.65	-103.63	2195	2	-0.89	-0.1	0.79	14
ODP 847	0.25	-95.30	3334	3	-1.05	0.57	1.62	30
RC11-210	1.80	-140.00	4400	2	-1.30	-0.09	1.21	14
ODP 851	2.75	-110.50	3760	2	-1.05	-0.05	1.00	31
Y69-106P	3.00	-86.50	2900	2	-1.95	-0.4	1.55	14
Mean -4°-3°N	-0.24				-1.01	0.29	1.29	
BNFC43	10.50	-109.00	2900	1	-1.80	-0.22	1.58	14

References are 1. Arz et al. [1999]; 2. Duerkoop et al. [1997]; 3. Mix and Ruddiman [1985]; 4. Curry and Crowley [1987]; 5. Oppo and Fairbanks [1989]; 6. Broecker [1986]; 7. Imbrie et al. [1973]; 8. Emiliani [1955]; 9. Slowey and Curry [1992]; 10. Stott and Tang [1996]; 11. Imbrie et al. [1984]; 12. McInyre et al. [1989]; 13. Wang et al. [1995]; 14. Shackleton [1977]; 15. Schneider et al. [1995]; 16. Anderson et al. [1989]; 17. Haddad et al. [1993]; 18. Kroon et al. [1993]; 19. Le and Shackleton [1992]; 20. Berger and Kiltingley [1977]; 21. Patrick and Thunell [1997]; 22. Berger et al. [1993]; 23. Schffelfein [1985]; 24. Thunell et al. [1994]; 25. Miao et al. [1994]; 26. Thunell et al. [1992]; 27. Schoenfeld and Kudrass [1993]; 28. Wang and Wang [1990]; 29. Chinzai et al. [1987]; 30. Farrell et al. [1995]; 31. Cannariato and Ravello [1997].

habitat [e.g., Hemleben et al., 1989]. In particular, *G. sacculifer* with a sac-like final chamber calcifies deeper in the water column and may therefore underestimate surface temperatures. In order to obtain a larger data set, however, we have combined both *G. sacculifer* morphotypes.

We calculate predicted  $\delta^{18}\text{O}_c$  values from  $\delta^{18}\text{O}_w$  and SST, using the paleotemperature equation by Epstein et al. [1953] in accordance with Fairbanks et al. [1992], the source of  $\delta^{18}\text{O}_c$  data for the Atlantic. In the Atlantic we compare the LH *G. sacculifer* and *G. ruber*  $\delta^{18}\text{O}$  values to  $\delta^{18}\text{O}_c$  within each region (Figure 4). In the Pacific, we compare *G. sacculifer*  $\delta^{18}\text{O}$  values to  $\delta^{18}\text{O}_c$  values derived from the  $\delta^{18}\text{O}_c/\sigma_t$  regression shown in Figure 2 because of a lack of adequate  $\delta^{18}\text{O}_w$  data to calculate more spatially resolved  $\delta^{18}\text{O}_c$  values (Figure 6). *G. ruber*  $\delta^{18}\text{O}$  values are on average lower than those of *G. sacculifer* (-0.4‰ [Deuser, 1987]). We add 0.4‰ to *G. ruber*  $\delta^{18}\text{O}$  values to account for this difference.

In the Atlantic we selected cores with sedimentation rates in excess of 2 cm kyr<sup>-1</sup> that lie above 3700 m in order to minimize bias of the isotopic signal due to bioturbation and shoaling of the glacial lysocline [Curry and Lohmann, 1986]. In the Pacific, dissolution tends to bias the core top samples; the glacial lysocline, on the other hand, is relatively deep, and calcite preservation is better than during the interglacial intervals [e.g., Farrell and Prell, 1991]. A comparison with modern ocean hydrography will show the extent to which foraminiferal  $\delta^{18}\text{O}$  values reflect the modern conditions in this ocean basin.

At all sites, LH and LGM data were chosen on the basis of  $\delta^{18}\text{O}$  stratigraphy and/or <sup>14</sup>C dating as provided in the original literature. There are inherent uncertainties in this approach; not all data chosen for the LH or LGM time splices may be truly contemporary or representative of these climatic extremes [e.g., Broecker et al., 1999]. In fact, much of the data scatter could stem from grouping data of differing ages. Because our major conclusions do not rely on observations made from single data points, age discrepancies do not significantly affect the findings of this study.

### 3. Results

#### 3.1 Atlantic

Meridional density gradients in the western, central, and eastern Atlantic are largely similar to the more generalized curve depicted in Figure 3 (Figures 4a-4c). All have a minimum at ~5°N, but the rate of density increase with latitudes differs. For example, in the western Atlantic the Northern Hemisphere has markedly lower density in comparison to the south, reflecting the disproportional larger amount of warm water advected to the north in the western boundary current. In the eastern Atlantic (Figure 4c), density increases rapidly with latitude, reflecting the relatively cool and dense waters flowing toward the equator within the eastern boundary currents.

Meridional profiles of the  $\delta^{18}\text{O}$  values of predicted calcite reflect the density gradients well (Figures 4d-4f). This is to be expected because there are ample sea water  $\delta^{18}\text{O}_w$  measurements to determine  $\delta^{18}\text{O}_c$  with a high degree of spatial resolution [Fairbanks et al., 1992]. For example, in the northwest the  $\delta^{18}\text{O}$  gradient is steep, in good agreement with the local

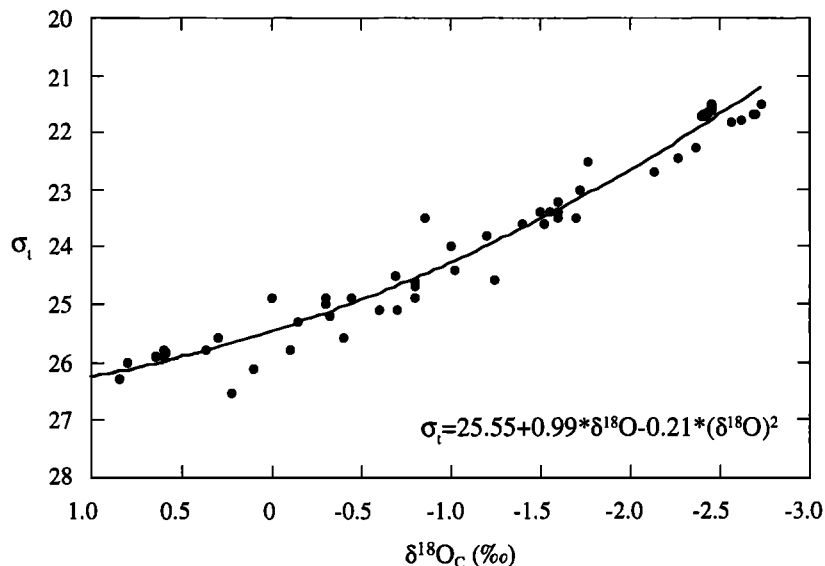


**Figure 2.** Correlation between  $\delta^{18}\text{O}$  values of predicted calcite ( $\delta^{18}\text{O}_c$ ) and  $\sigma_t$  ( $\sigma_t$  is density minus  $1000 \text{ kg m}^{-3}$ ) [Levitus and Boyer, 1994] in the tropical to subtropical surface oceans between  $40^\circ\text{N}$  and  $40^\circ\text{S}$ . Atlantic  $\delta^{18}\text{O}_c$  values are from Fairbanks *et al.* [1992] interpolated along three longitudinal transects ( $20^\circ\text{W}$ ,  $30^\circ\text{W}$ , and  $40^\circ\text{W}$ ) at increments of  $10^\circ$  latitude. Pacific and Indian Ocean  $\delta^{18}\text{O}_c$  were derived using the paleotemperature equation of Epstein *et al.* [1953] with Geochemical Ocean Sections Study (GEOSECS) sea water  $\delta^{18}\text{O}_w$  values ( $\delta^{18}\text{O}_w$ ) and temperatures. Additional data for the western equatorial Pacific were calculated from  $\delta^{18}\text{O}_w$  values of Fairbanks *et al.* [1997], temperatures from Levitus and Boyer [1994], and the paleotemperature equation of Epstein *et al.* [1953].

density gradient (Figures 4a and 4d). In the central and eastern Atlantic the meridional  $\delta^{18}\text{O}$  gradient is symmetrical about  $5^\circ\text{N}$ , in excellent agreement with the shape of the modern density gradient (Figures 4e and 4f).

With few exceptions, planktonic foraminiferal  $\delta^{18}\text{O}$  values (*G. ruber*  $+0.4\text{‰}$  and *G. sacculifer*) from the late Holocene

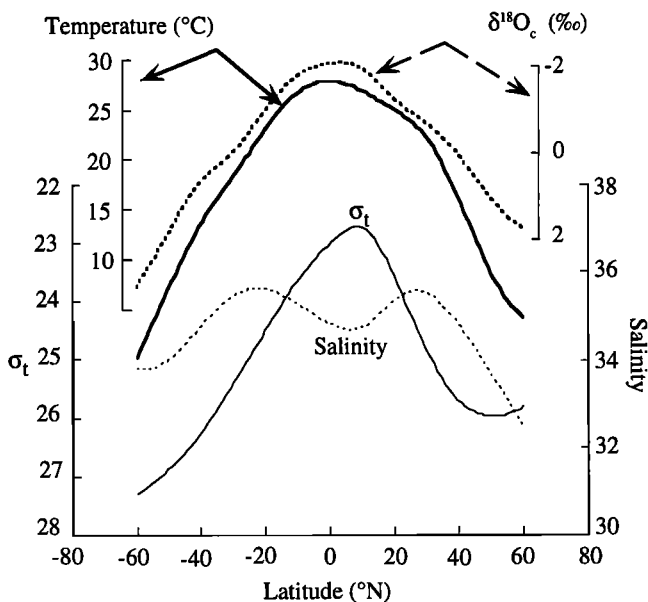


**Figure 3.** Averaged Pacific and Atlantic meridional gradients in temperature, salinity,  $\sigma_t$ , and  $\delta^{18}\text{O}$  values of predicted calcite ( $\delta^{18}\text{O}_c$ ) (modified from Pickard and Emery [1990]). The  $\delta^{18}\text{O}_c$  data were calculated using the paleotemperature equation of Epstein *et al.* [1953] with  $\delta^{18}\text{O}_w$  values estimated from Schmidt [1999].

follow the  $\delta^{18}\text{O}_c$  gradients, and hence density gradients, well (Figures 4d-4f). Low density that characterizes the northwestern Atlantic today is expressed by low planktonic foraminiferal  $\delta^{18}\text{O}$  values in comparison to values in the north central and northeastern regions. Foraminiferal  $\delta^{18}\text{O}$  values also reproduce the relatively steep density gradient in the northeastern Atlantic, even though values between  $18^\circ\text{N}$  and  $20^\circ\text{N}$  appear to be too low by  $\sim 0.5\text{-}1\text{‰}$  (Figure 4f). We suspect that relatively low  $\delta^{18}\text{O}$  values in this region do not represent an annual signal but rather growth during the nonupwelling, warm season [Deuser *et al.*, 1981; Deuser, 1987].

In the glacial ocean, meridional  $\delta^{18}\text{O}$  gradients are largely similar to those of the late Holocene, although important differences exist. The zonal  $\delta^{18}\text{O}$  gradient in the Northern Hemisphere was reduced with respect to the late Holocene as evidenced by  $\delta^{18}\text{O}$  values in the glacial northwestern Atlantic as high as in the central and eastern regions (Figure 4d). Moreover, the entire northern subtropics underwent more extreme glacial to interglacial shifts in surface ocean hydrography than equivalent latitudes in the Southern Hemisphere. The planktonic foraminifera display a trend of increasingly higher glacial  $\delta^{18}\text{O}$  values toward the north (Figures 4d-4f); however, the data scatter is large. Relatively large data scatter is not surprising given the number of environmental and ecological variables that can affect foraminiferal  $\delta^{18}\text{O}$  values [e.g., Mulitza *et al.*, 1998; Lohmann, 1995; Fairbanks and Wiebe, 1980; Ravelo and Fairbanks, 1992; Bouvier-Soumagnac *et al.*, 1986; Spero and DeNiro, 1987] in addition to analytical discrepancies between laboratories and temporal uncertainties.

In order to better illustrate the LGM versus LH differences in meridional  $\delta^{18}\text{O}$  gradients we have averaged values from adjacent sites (for each species separately; see Table 1) and then calculated their glacial to interglacial  $\delta^{18}\text{O}$  amplitude



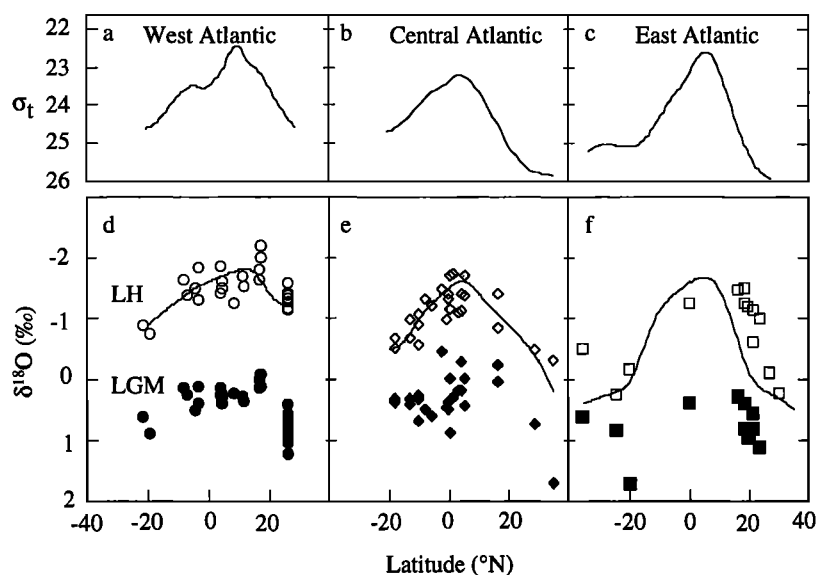


**Figure 4.** (a-c) Meridional gradients in  $\sigma_t$  and corresponding *G. ruber* and *G. sacculifer*  $\delta^{18}O$  values (combined) from the late Holocene (LH) (open symbols) and Last Glacial Maximum (LGM) (solid symbols) in the (d) the western, (e) central, and (f) eastern Atlantic. The solid line through the LH values denotes the meridional gradient in  $\delta^{18}O_c$  within each region (see section 2 for an explanation).

( $\Delta\delta^{18}O$ ) (Figure 5a). A clear trend emerges of increasing  $\Delta\delta^{18}O$  with north latitude (Figure 5a). In the southern subtropics, a minimum change of  $\sim 1\text{‰}$  approximates the  $\delta^{18}O$  shift of  $\sim 1\text{‰}$  that can be ascribed to change in global ice volume alone. In the northern subtropics the maximum  $\Delta\delta^{18}O$  amplitude of  $2\text{‰}$  far exceeds the magnitude of global ocean reservoir changes. These observations suggest that beyond global ocean density increases the southern subtropical sea surface density varied relatively little between the two climatic extremes, while the northern subtropical sea surface density increased (Figure 5b). Little change in foraminiferal  $\delta^{18}O$  values above the whole ocean background would also suggest insignificant additional local density variability. Therefore we can assess local or regional hydrographic changes by subtracting  $1\text{‰}$  from LGM  $\delta^{18}O$  values to account for the ice volume effect leaving a residual local  $\delta^{18}O$  signal from which we calculate the corresponding surface density (using the regression given in Figure 2). In this scenario, no change in relative density occurred in the Southern Hemisphere, where the  $\Delta\delta^{18}O$  of the foraminifera was  $\sim 1\text{‰}$ . In the northern subtropics, on the other hand, the surface water density increased by between  $0.75 \text{ kg m}^{-3}$  and  $1.5 \text{ kg m}^{-3}$  (Figure 5b). The magnitude of this density change is significant; it is comparable to the seasonal density contrast in the central North Atlantic at  $25^{\circ}\text{N}$  [Levitus and Boyer, 1994]. A different approach would be to account for LGM ocean density changes due to a higher ocean salt content (assuming LH average salinity of 35.0 and LGM average salinity of 36.2). While the absolute values of the change in density derived in this manner are generally higher by as much as a factor of 2 (not shown), the nature of the density gradients is the same.

### 3.2. Pacific

Meridional density profiles in the Pacific are largely similar to those in the Atlantic with minima just north of the

equator and relatively steep gradients toward the poles (Figure 7). As in the Atlantic, regional differences are important. In the westernmost subtropical North Pacific, the South China and Sulu Seas region ( $\sim 10^{\circ}\text{N}$  and  $120^{\circ}\text{E}$ ), density is particularly low, reflecting the relatively high amount of rainfall received in this region because of the strong influence of the Indonesian low-pressure cell [Peixoto and Oort, 1992] (Figure 6a). In the eastern equatorial Pacific, between  $\sim 5^{\circ}\text{S}$  and  $0^{\circ}$ , the density plateau (Figure 6b) reflects the effect of upwelling of cooler and more dense subsurface water within the equatorial cold tongue.

Late Holocene *G. sacculifer*  $\delta^{18}O$  values from the Pacific agree well with the modern density (and corresponding  $\delta^{18}O_c$ ) gradients even though the foraminiferal data scatter is large (Figures 6c and 6d). Foraminiferal  $\delta^{18}O$  values decrease rapidly from  $35^{\circ}\text{S}$  toward the equator in the western Pacific, in agreement with the slope of the density ( $\delta^{18}O_c$ ) gradient (Figure 6a). Furthermore, extremely low  $\delta^{18}O$  values are recorded by foraminifera from the South China and Sulu Seas region ( $\sim 10^{\circ}\text{N}$  and  $120^{\circ}\text{E}$ ), in agreement with the low surface water density characterizing this region. Excellent agreement between LH  $\delta^{18}O$  values and the modern density ( $\delta^{18}O_c$ ) gradient also exists in the eastern Pacific where the foraminiferal  $\delta^{18}O$  values increase from the southern subtropics toward  $10^{\circ}\text{S}$ , remain relatively constant across the equator, and then decrease toward  $20^{\circ}\text{N}$  in accord with the modern density ( $\delta^{18}O_c$ ) gradient (Figures 6b and 6d). The agreement between late Holocene  $\delta^{18}O$  values and the modern hydrography, particularly in the east, is encouraging because it suggests that the meridional gradients have not been masked significantly by low sedimentation rates and carbonate dissolution.

In the glacial Pacific the familiar trend of increasingly higher  $\delta^{18}O$  values with north latitude prevailing in the Atlantic is also apparent (Figure 6). Again we use average

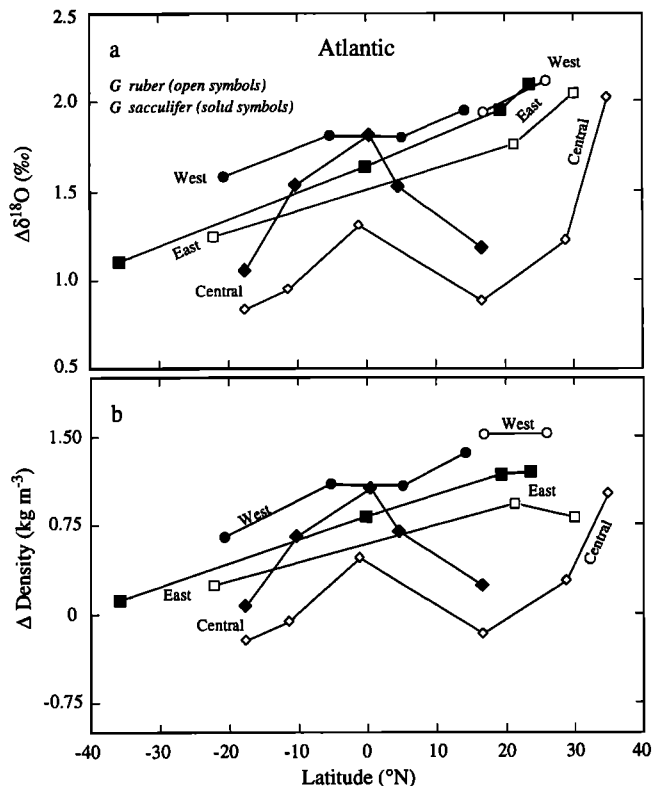


**Figure 5.** (a) Meridional gradients in glacial to interglacial amplitude in the *G. ruber* and *G. sacculifer*  $\delta^{18}\text{O}$  values ( $\Delta\delta^{18}\text{O}$ ) from the Atlantic. The  $\Delta\delta^{18}\text{O}$  values were calculated by first grouping data from adjacent sites and then calculating the difference between LH and LGM  $\delta^{18}\text{O}$  data (Table 1). (b) Meridional gradients in the glacial to interglacial amplitude of surface water density changes above whole ocean density changes. Little change in foraminiferal  $\delta^{18}\text{O}$  values above the whole ocean background suggests little additional local density variability. Therefore we assess local or regional hydrographic changes by subtracting 1‰ from LGM  $\delta^{18}\text{O}$  values to account for the ice volume effect leaving a residual local  $\delta^{18}\text{O}$  signal from which we calculate the corresponding LGM surface density (using the regression given in Figure 2 and plotting the LGM-LH density difference). Hence the 1‰ mark on the  $\Delta\delta^{18}\text{O}$  scale (Figure 5a) corresponds to the 0  $\text{kg m}^{-3}$  mark on the density scale.

values to highlight these trends (Figure 7a). In the western subtropics the  $\Delta\delta^{18}\text{O}$  amplitude increases from  $\sim 1\text{‰}$  at  $30^{\circ}\text{S}$  to almost  $2\text{‰}$  at  $30^{\circ}\text{N}$  (Figure 7a). In the eastern Pacific,  $\Delta\delta^{18}\text{O}$  values increase from  $0.75\text{‰}$  at  $25^{\circ}\text{S}$  to  $1.5\text{‰}$  at  $10^{\circ}\text{N}$ . As in the Atlantic, minimum  $\Delta\delta^{18}\text{O}$  values recorded in the southern subtropics are close to the global ocean  $\delta^{18}\text{O}$  shift of  $1\text{‰}$  due to the ice volume effect, while a maximum amplitude of  $\sim 2\text{‰}$  in the Northern Hemisphere suggests that significant changes took place in local surface water hydrography.

In the eastern Pacific, it is possible that the meridional  $\Delta\delta^{18}\text{O}$  gradients have been affected in part by low sedimentation rates, corrosive bottom water, and the associated bias toward higher core top  $\delta^{18}\text{O}$  values. Sedimentation rates tend to be highest at the equator (e.g., Table 1), and we would expect that the amplitude of the glacial to interglacial  $\delta^{18}\text{O}$  signal is larger than at sites to the north and south. Particularly low sedimentation rates ( $\sim 1 \text{ cm kyr}^{-1}$ ) characterize three of the southern sites as well as the most

northern site (Table 1). The relatively small amplitude in Southern Hemisphere  $\Delta\delta^{18}\text{O}$  shift may in part be due to a relatively high degree of dissolution among the core top assemblages. At  $10^{\circ}\text{N}$  a relatively high  $\Delta\delta^{18}\text{O}$  value is apparent despite the low sedimentation rates; it might actually underestimate the true climate signal in this region. We are confident that the  $\Delta\delta^{18}\text{O}$  gradient toward northern latitudes between the equator and  $10^{\circ}\text{N}$  is real and reflects an increase in the local density of surface waters in the Northern Hemisphere in comparison to sites at equivalent latitudes in the southern hemisphere. Low sedimentation rates and dissolution do not plague our interpretations from the western Pacific (or Atlantic) because they do not vary systematically with latitude (Table 1). They do, however, hamper discussions about glacial to interglacial changes in the zonal  $\delta^{18}\text{O}$  gradients between ocean basins and within the Pacific.

Following the example from the Atlantic, we have calculated the glacial to interglacial amplitude in surface water density after accounting for whole ocean changes due to polar freshwater storage ( $\Delta$  density, Figure 7b). Results suggest that the residual density of the southern subtropical regions remained the same between the glacial to interglacial climate states. In the northern subtropics the relative density increased by as much as  $1.7 \text{ kg m}^{-3}$  in the South China Sea region, by  $\sim 1 \text{ kg m}^{-3}$  farther north, and by  $0.75 \text{ kg m}^{-3}$  in the east at  $10^{\circ}\text{N}$  (Figure 7b). For comparison, the seasonal density at these sites varies by  $0.9 \text{ kg m}^{-3}$ ,  $3 \text{ kg m}^{-3}$ , and  $0.3 \text{ kg m}^{-3}$ , respectively [Levitus and Boyer, 1994] (Table 2).

We use the seasonal analogue to attempt a diagnosis of glacial to interglacial changes in surface water density. In the South China Sea, seasonality is dominated by salinity changes (Table 2). Hence we speculate that the glacial to

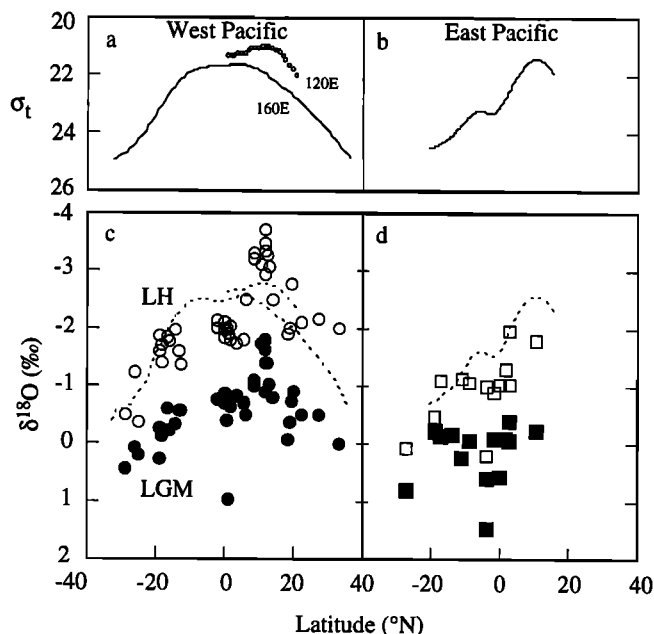


**Figure 6.** (a-b) Meridional gradients in  $\sigma_t$  and corresponding *G. sacculifer*  $\delta^{18}\text{O}$  values from the LH (open symbols) and LGM (solid symbols) in the (c) western, and (d) eastern Pacific. Dashed lines through the LH values represent  $\delta^{18}\text{O}_e$  calculated from the regression in Figure 2 (see section 2 for an explanation).

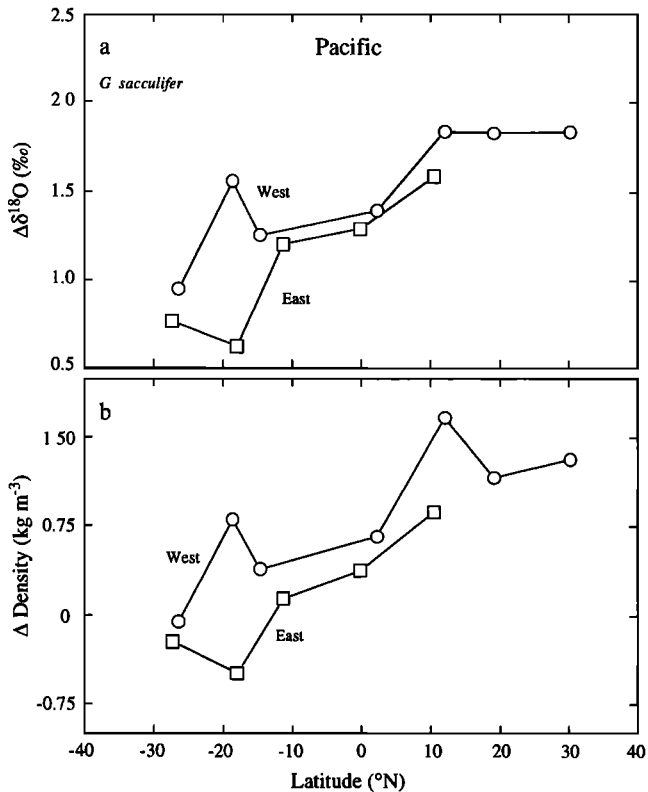


**Figure 7.** (a) Meridional gradients in glacial to interglacial amplitude in *G. sacculifer*  $\delta^{18}\text{O}$  values ( $\Delta\delta^{18}\text{O}$ ) from the Pacific. (b) Meridional gradients in the glacial to interglacial amplitude of surface water density estimates. See Figure 5 for details.

interglacial density contrast stems from a higher glacial sea surface salinity in accordance with previous findings from the region [e.g., Martinez *et al.*, 1997]. This scenario would be consistent with reduced net freshwater fluxes from the Atlantic to the Pacific and more arid tropics during the LGM. At 30°N, seasonal temperature changes are large, while salinity remains relatively constant (Table 2). It seems likely that on glacial to interglacial timescales temperature changes dominate the density properties as well. In the east at 10°N, a region which lies within the expanse of relatively warm and fresh tropical surface water that extends westward from the coast of Costa Rica [Wyrki, 1966], neither temperature nor salinity vary appreciably between the cold and warm season. In this case the seasonal analogue provides no basis for speculation about the significance of past temperature versus salinity changes.

#### 4. Discussion

Our compilation of planktonic foraminiferal  $\delta^{18}\text{O}$  values suggests that during the LGM, more extreme changes in surface hydrography occurred in the northern tropical to subtropical regions than at equivalent latitudes in the Southern Hemisphere. In the Atlantic a cooling of the sea surface is not surprising given the relative proximity of a large North American and Greenland ice sheet. In the Pacific, however, it is unlikely that a more distant Northern Hemisphere ice mass exerted as great a direct temperature control on the tropical to subtropical sea surface. Regardless of the cause, the relatively high density in the northern subtropical regions may have important implications on the structure of the tropical thermocline because thermocline water originates at subtropical latitudes. Thermocline waters are produced by Ekman pumping in regions of maximum wind stress curl (e.g., 30°N and 30°S) and by buoyancy fluxes when surface waters cool during the winter in either hemisphere [e.g., Tsuchiya *et al.*, 1989]. Climate conditions at the sea surface at latitudes of isopycnal outcropping can affect the vertical structure (e.g., depth and/or intensity) of the tropical thermocline [Luyten *et al.*, 1983; Bleck *et al.*, 1989; Liu and Pedloski, 1994, Slowey and Curry, 1995]. For example, a shift in the latitude of thermocline water production may affect the depth to which waters can sink and therefore the vertical structure of the tropical thermocline. In turn, such changes could modify the thermal structure of the tropical surface ocean by decreasing or increasing the temperature of source waters to the tropical ocean upwelling regimes [Luyten *et al.*, 1983]. In addition, the strength of subtropical winds can influence thermocline stratification by changing the amount of Ekman downwelling and hence the amount of relatively warm surface waters feeding the tropical thermocline [Liu and Philander, 1995].

In the Atlantic the relatively large increase in foraminiferal  $\delta^{18}\text{O}$  values toward northern latitudes leads us to believe that the region of thermocline water formation may have migrated or expanded toward the equator. Steeper subtropical density gradients in the North Atlantic are consistent with previous studies which have shown that during the LGM the position of the northern polar front, which is associated with the boundary between the Atlantic subtropical and subpolar gyre, was located farther south and in a more zonal position than today [e.g., Ruddiman and McIntyre, 1976; *Climate: Long-Range Investigation, Mapping, and Prediction (CLIMAP) Project Members*, 1981]. Most likely, the polar front was forced toward the south by the growth of a large continental ice sheet modifying the westerly wind field [Kutzbach and

**Table 2.** Summary of Seasonal Changes in North Pacific Subtropical Sea Surface Hydrography

	Temperature <sup>a</sup> , °C	Salinity <sup>a</sup>	Density <sup>b</sup> , kg m <sup>-3</sup>
South China Sea (10°N, 120°E)	29.5-27.5	33.0-33.6	1020.4-1021.5
Northwest (30°N, 160°E)	26-18	34.5-34.8	1022.0-1025.1
Northeast (10°N, 110°W)	28-27	34.2-34.2	1021.8-1022.1

<sup>a</sup>Data from Levitus and Boyer [1994].

<sup>b</sup>Density was calculated from temperature and salinity using the international equation of state of sea water [UNESCO, 1981].

Guetter, 1986]. Consequently, the locations of Ekman upwelling (e.g., in the subpolar gyre) and downwelling (e.g., in the subtropical gyre) became more zonal and shifted to the south [Kefffer *et al.*, 1988]. If these reconstructions are correct, they should imply a more compressed subtropical gyre than today and steeper temperature gradients in the middle to low latitudes. A reconstruction of the upper ocean vertical temperature profile in the western Atlantic provides evidence that ventilation of the glacial subtropical thermocline was indeed stronger and that the thermal gradient across the thermocline was steeper [Slowey and Curry, 1992, 1995]. The spatial distribution of glacial age planktonic foraminiferal  $\delta^{18}\text{O}$  values in the Atlantic lend support to these studies.

In contrast to the Atlantic, in the Pacific the tropical thermocline is predominantly ventilated from the south. Salinity measurements indicate that 50-75% of the equatorial thermocline water originates in the Southern Hemisphere with smaller contributions from the north [Tsuchiya *et al.*, 1989]. This is, in part, because the Intertropical Convergence Zone (at  $\sim 5^\circ\text{N}$ , on average) poses a barrier to water mass exchange and favors ventilation from the south. In addition, Southern Hemisphere ventilation dominates because the North Pacific thermocline loses water through the Indonesian Throughflow which must be balanced by cross-equatorial advection from the Southern Hemisphere [Rodgers *et al.*, 1999].

Distinct north-to-south, cross-equatorial gradients exist in the temperature and salinity of thermocline water. Along isopycnals, Southern Hemisphere water tends to be warmer and more saline than northern component source waters owing to differences in freshwater fluxes at the sea surface [e.g., Tsuchiya *et al.*, 1989; Rodgers *et al.*, 1999]. Varying the proportion of Northern versus Southern Hemisphere source waters to the tropical thermocline offers a mechanism that can influence the structure of the tropical thermocline and the temperature and salinity of the upwelling water [Rodgers *et al.*, 1999]. Furthermore, it has been argued and illustrated in numerical ocean models that temperature anomalies set in the regions of thermocline outcropping in the North Pacific can be propagated down and toward the equator where they may contribute to the temperature anomalies of upwelled water [Deser *et al.*, 1996; Gu and Philander, 1997; Zhang *et al.*, 1998]. While such a process hinges on the assumption that the Pacific thermocline is a closed system, it is intriguing because it implies an extratropical forcing of tropical climates.

Our compilation from the Pacific is critical because unlike in the Atlantic, no data exist to directly reconstruct the three-dimensional nature of the thermocline in the subtropical regions, and only little information is available on thermocline stratification during the LGM [Ravelo and Shackleton, 1995; Patrick and Thunell, 1997]. Therefore we must rely on the meridional surface density gradients as a recorder of subsurface processes. Our results provide strong evidence for a significant increase in the density of Northern Hemisphere subtropical surface water. Without a significant source of freshwater input to the western subtropics (and generally lower SST), the northern limb of the North Pacific gyre was more dense than today. We speculate that during the LGM the proportion of Northern Hemisphere water sinking into the tropical thermocline was increased with respect to

today. A relative increase in Northern Hemisphere thermocline water source relative to Southern Hemisphere sources would affect the thermal structure of the tropical thermocline and lower the temperature of the upwelling water along the equator. A relative increase in northern subtropical sea surface density may also have presented favorable conditions for enhanced intermediate water ventilation in the glacial North Pacific [Keigwin, 1998]. Furthermore, relatively high North Pacific salinities reduced the Atlantic to Pacific salinity gradient, which may have affected North Atlantic deep water production rates during the LGM [Broecker, 1989, 1991]. While speculative at the moment, these predictions could be tested in numerical ocean models such as those that assess the structure of the tropical thermocline specifically and sea surface temperature and LGM climate changes more generally [e.g., Bush and Philander, 1998; Gu and Philander, 1997; Zhang *et al.*, 1998; Ganapolski *et al.*, 1998].

In addition, our compilation has important applications for numerical modeling of ocean and atmospheric circulation. The interhemispheric asymmetry evidenced by foraminiferal  $\delta^{18}\text{O}$  values provides a specific test for glacial boundary conditions such as sea surface temperatures and water vapor transports. For example, in combination, specified temperature and salinity values should resemble the observed increase in Northern Hemisphere surface water density. Conversely, glacial climate model output needs to correctly reproduce the asymmetry of the meridional density gradient. Furthermore, our compilation provides a very direct test for modelers who integrate climate signal modeling with observations from the sediment record [e.g., Schmidt, 1999].

## 5. Conclusions

We have compiled published planktonic foraminiferal oxygen isotope values from the tropical to subtropical Atlantic and Pacific for the late Holocene and the Last Glacial Maximum. Our compilation suggests that during the LGM, more extreme changes in surface ocean density occurred in the northern tropical to subtropical regions than at equivalent latitudes in the Southern Hemisphere. In the Atlantic the results support prior reconstructions of LGM surface ocean hydrography and thermocline ventilation, suggesting a more compressed Northern Hemisphere subtropical gyre. In the Pacific this interhemispheric asymmetry is more likely a phenomenon of significantly reduced freshwater fluxes to the northern tropics and subtropics. The increase in surface ocean density in this region has implications for thermocline ventilation, suggesting that the proportion of Northern Hemisphere source waters to the tropical thermocline was greater during the LGM than it is today. We speculate that a greater Northern Hemisphere thermocline water source would also cool the waters upwelling in the equatorial Pacific, which might be testable with numerical ocean models.

**Acknowledgments.** We thank Tom Guilderson, who generously provided his compilation of planktonic foraminiferal  $\delta^{18}\text{O}$  values to augment our own efforts. Reviews by J. Lynch-Stieglitz and L. Labyrie as well as comments by M. Delaney substantially improved this manuscript. This study was supported by an NSF sponsored postdoctoral fellowship to K. B. and by NSF OCE-9733688 (D. P. S.).

## References

- Anderson, D. M., W. L. Prell, and N. J. Barratt, Estimates of sea surface temperatures in the Coral Sea at the Last Glacial Maximum, *Paleoceanography*, 4, 615-627, 1989.
- Arz, H. W., J. Paetzold, and G. Wefer, The deglacial history of the western tropical Atlantic as inferred from high resolution stable isotope records off northeastern Brazil, *Earth Planet. Sci. Lett.*, 167, 105-117, 1999.
- Berger, W. H., and J. S. Killingly, Glacial-Holocene transition in deep-sea carbonates: Selective dissolution and the stable isotope signal, *Science*, 197, 563-566, 1977.
- Berger, W. H., T. Bickert, H. Schmidt, and G. Wefer, Quaternary oxygen isotope record of pelagic foraminifers: Site 806 Ontong-Java Plateau, *Proc. Ocean Drill. Program, Sci. Results*, 130, 381-395, 1993.
- Billups K., and H. J. Spero, Reconstructing the stable isotope geochemistry and paleotemperatures of the equatorial Atlantic During the Last 150,000 years: Results from individual foraminifera, *Paleoceanography*, 11, 217-238, 1996.
- Bleck, R., H. P. Hanson, D. Hu, and E. B. Kraus, Mixed layer-thermocline interaction in a three-dimensional isopycnic coordinate model, *J. Phys. Oceanogr.*, 19, 1417-1439, 1989.
- Bouvier-Soumagnac, Y., J. Duplessy, and A. H. Bé, Isotopic composition of laboratory cultured planktonic foraminifer: Implications for paleoclimatic reconstructions, *Oceanol. Acta*, 9, 519-522, 1986.
- Broecker, W. S., Oxygen isotope constraints on surface ocean temperatures, *Quat. Res.*, 26, 121-34, 1986.
- Broecker, W. S., The salinity contrast between the Atlantic and Pacific Oceans during glacial times, *Paleoceanography*, 4, 207-212, 1989.
- Broecker, W. S., The great ocean conveyor, *Oceanography*, 4, 79-89, 1991.
- Broecker, W. S., K. Matsumoto, E. Clark, I. Hadjas, and G. Bonani, Radiocarbon differences between coexisting foraminiferal species, *Paleoceanography*, 14, 431-436, 1999.
- Bush, A. B. G., and S. G. H. Philander, The role of ocean-atmosphere interactions in tropical cooling during the Last Glacial Maximum, *Science*, 279, 1341-1344, 1998.
- Cannariato, K. G., and A. C. Ravelo, Plio-Pleistocene evolution of eastern tropical Pacific surface water circulation and thermocline depth, *Paleoceanography*, 12, 805-820, 1997.
- Chinzei, K., K. Fujioka, H. Kitazato, I. Koizumi, T. Oba, M. Oda, H. Okada, T. Sakai, and Y. Tanimura, Postglacial environmental change of the Pacific ocean off the coast of central Japan, *Mar. Micropaleontol.*, 11, 273-291, 1987.
- Climate: Long-Range Investigation, Mapping, and Prediction (CLIMAP) Project Members, Seasonal reconstruction of the Earth's surface during the Last Glacial Maximum, *Map Chart Ser.*, 36, Geol. Soc. of Am., Boulder, Colo., 1981.
- Craig, H., and L. I. Gordon, Isotopic oceanography: Deuterium and oxygen 18 variations in the ocean and marine atmosphere, in *Stable Isotope Studies in Oceanographic Studies and Paleotemperatures*, edited by D. R. Schink and J. T. Corless, Univ. of R. I., Kingston, 1965.
- Curry, W. B., and T. J. Crowley, The  $\delta^{13}\text{C}$  of equatorial Atlantic surface waters: Implications for ice age  $\text{CO}_2$  levels, *Paleoceanography*, 2, 489-517, 1987.
- Curry, W. B., and G. P. Lohmann, Late Quaternary carbonate sedimentation at the Sierra Leone Rise, *Mar. Geol.*, 70, 223-250, 1986.
- Curry, W. B., and D. W. Oppo, Synchronous, high-frequency oscillations in tropical sea surface temperatures and North Atlantic Deep Water production during the last glacial cycle, *Paleoceanography*, 12, 1-14, 1997.
- Deser, C., M. A. Alexander, and M. S. Timlin, Upper-ocean thermal variations in the North Pacific during 1970-1991, *J. Clim.*, 9, 1840-1855, 1996.
- Deuser, W. G., Seasonal variability in the isotopic composition and deep-water fluxes of the tests of perennially abundant planktonic foraminifera of the Sargasso Sea: Results from sediment-trap collections and their paleoceanographic significance, *J. Foraminiferal Res.*, 17, 14-27, 1987.
- Deuser, W. G., E. H. Ross, C. Hemleben, and M. Spindler, Seasonal changes in species composition, numbers, mass, size, and isotopic composition of planktonic foraminifera settling into the deep Sargasso Sea, *Paleogeogr. Paleoclimatol.*, 33, 103-127, 1981.
- Dürkoop, A., W. Hale, S. Mulitza, J. Paetzold, and G. Wefer, Late Quaternary variations of sea surface salinity and temperature in the western tropical Atlantic: Evidence from  $\delta^{18}\text{O}$  of *Globigerinoides sacculifer*, *Paleoceanography*, 12, 764-772, 1997.
- Emiliani, C., Pleistocene temperatures, *J. Geology*, 63, 538-578, 1955.
- Epstein, S., R. Buchsbaum, H. A. Lowenstam, and H. C. Urey, Revised carbonate-water isotopic temperature scale, *Geol. Soc. Am. Bull.* 64, 1315-1326, 1953.
- Eshel, G., D. P. Schrag, and B. F. Farrell, Troposphere-planetary boundary layer interactions and the evolution of ocean surface density: Lessons from Red Sea Corals, *J. Climate*, in press, 1999.
- Fairbanks, R. G., and P. H. Wiebe, Foraminifera and chlorophyll maximum: Vertical distribution, seasonal succession, and paleoceanographic significance, *Science*, 209, 1524-1526, 1980.
- Fairbanks R. G., C. D. Charles, and J. D. Wright, Origin of global meltwater pulses, in *Radiocarbon After Four Decades*, edited by R. E. Taylor, pp. 473-500, Springer-Verlag, New York, 1992.
- Fairbanks, R. G., M. N. Evans, J. L. Rubenstone, R. A. Mortlock, K. Broad, M. D. Moore, and C. D. Charles, Evaluating climate indices and their geochemical proxies measured in corals, *Coral Reefs*, 16, S93-S100, 1997.
- Farrell, J. W., and W. L. Prell, Pacific,  $\text{CaCO}_3$  preservation and  $\delta^{18}\text{O}$  since 4 Ma: Paleoceanographic and paleoclimatic implications, *Paleoceanography*, 6, 485-498, 1991.
- Farrell, J. W., D. W. Murray, V. S. McKenna, and A. C. Ravelo, Upper ocean temperature and nutrient contrasts inferred from Pleistocene planktonic foraminifer  $\delta^{18}\text{O}$  and  $\delta^{13}\text{C}$  in the eastern equatorial Pacific, *Proc. Ocean Drill. Program, Sci Results*, 133, 289-320, 1995.
- Ganapolski, A., S. Rahmstorf, V. Petoukhov, and M. Claussen, Simulations of modern and glacial climates with a coupled global model of intermediate complexity, *Nature*, 391, 351-356, 1998.
- Gu, D., and S. G. H. Philander, Interdecadal climate fluctuations that depend on exchanges between the tropics and extratropics, *Nature*, 275, 805-807, 1997.
- Haddad, G. A., A. W. Droxler, D. Kroon, and D. W. Müller, Quaternary  $\text{CaCO}_3$  input and preservation within the Antarctic intermediate water: Mineralogical and isotopic results from Holes 818B and 817A, Townsville trough (Northeastern Australia Margin), *Proc. Ocean Drill. Program, Sci Results*, 133, 203-226, 1993.
- Hemleben, C., M. Spindler, and O. R. Anderson, *Modern Planktonic Foraminifera*, 364 pp., Springer-Verlag, New York, 1989.
- Imbrie, J., J. van Donk, and N. G. Kipp, Paleoclimatic investigation of a late Pleistocene Caribbean deep-sea core: Comparison of isotopic and faunal methods, *Quat. Res.* 3, 10-73, 1973.
- Imbrie, J., J. Hays, J. D. Martinson, A. McIntyre, A. C. Mix, J. Morley, N. G. Pisias, W. L. Prell, and N. J. Shackleton, The orbital theory of Pleistocene climate; Support from a revised chronology of the marine  $\delta^{18}\text{O}$  records, in *Milankovitch and Climate: Understanding the Response to Astronomical Forcing*, vol. 1, edited by A. Berger et al., pp. 269-305, D. Reidel, Norwell, Mass., 1984.
- Keffer, T., D. G. Martinson, and B. H. Corliss, The position of the Gulf Stream during Quaternary glaciations, *Science*, 241, 440-442, 1988.
- Keigwin, L. D., Glacial-age hydrography of the far northwest Pacific Ocean, *Paleoceanography*, 13, 323-339, 1998.
- Kroon, D., I. Alexander, and K. Darling, Planktonic and benthic foraminiferal abundances and their ratios (P/B) as expressions of middle-late Quaternary changes in water mass distribution and flow intensity on the northeastern Australian Margin, *Proc. Ocean Drill. Program, Sci Results*, 133, 181-188, 1993.
- Kutzbach, J. E., and P. J. Guetter, The influence of changing orbital parameters on surface boundary conditions on climate simulations for the past 18,000 years, *J. Atmos. Sci.*, 43, 1726-1759, 1986.
- Le, J., and N. J. Shackleton, Carbonate dissolution fluctuations in the western equatorial Pacific cores, *Quat. Sci. Rev.*, 7, 21-42, 1992.
- Levitus, S., and T. P. Boyer, *World Ocean Atlas 1994*, vol. 4, *Temperature*, NOAA Atlas NESDIS 4, 129 pp., Nat. Oceanic and Atmos. Admin., Silver Spring, Md., 1994.
- Levitus, S., R. Burgett, and T. P. Boyer, *World Ocean Atlas 1994*, vol. 3, *Salinity*, NESDIS 3, 111 pp., Nat. Oceanic and Atmos. Admin., Silver Spring, Md., 1994.
- Liu, Z., and J. Pedloski, Thermocline forced by annual and decadal Surface temperature variation, *J. Phys. Oceanogr.*, 24, 587-608, 1994.
- Liu, Z., and S. G. Philander, How different wind stress patterns affect the tropical-subtropical circulations of the upper ocean, *J. Phys. Oceanogr.*, 25, 449-462, 1995.
- Lohmann, G. P., A model for variations in the chemistry of planktonic foraminifera due to secondary calcification and selective dissolution, *Paleoceanography*, 10, 445-458, 1995.
- Luyten, J. R., J. Pedlosky, and H. Stommel, The ventilated thermocline, *J. Phys. Oceanogr.*, 13, 292-309, 1983.
- Lynch-Stieglitz, J., B. C. Curry, and N. Slowey, A geostrophic transport estimate for the Florida Current from the oxygen isotope composition of benthic foraminifera, *Paleoceanography*, 14, 360-373, 1999.
- Martinez, J. I., P. De Dekker, and A. R. Chivas, New estimates for salinity changes in the western Pacific warm Pool during the last glacial maximum: Oxygen-isotope evidence, *Mar. Micropaleontol.*, 32, 311-340, 1997.
- McIntyre, A., W. F. Ruddiman, K. Karlin, and A. C. Mix, Surface water response to orbital forcing, *Paleoceanography*, 4, 19-55, 1989.
- Miao, Q., R. C. Thunell, and D. M. Anderson, Glacial-Holocene carbonate dissolution and sea surface temperatures in the South China and Sulu Seas, *Paleoceanography*, 9, 269-290, 1994.

- Mix, A. C., and W. F. Ruddiman, Structure and timing of the last deglaciation: Oxygen isotope evidence, *Quat. Sci. Rev.*, **4**, 59-108, 1985.
- Mulitza, S. M., T. Wolff, J. Paetzold, W. Hale, and G. Wefer, Temperature sensitivity of planktonic foraminifera and its influence on the oxygen isotope record, *Mar. Micropaleontol.*, **33**, 223-240, 1998.
- Norton, F. L., III, E. D. Hausman, and M. B. McElroy, Hydrospheric transports, the oxygen isotope records, and tropical sea surface temperatures during the Last Glacial Maximum, *Paleoceanography*, **12**, 15-22, 1997.
- Oppo, D. W., and R. G. Fairbanks, Carbon isotope composition of tropical surface water during the past 22,000 years, *Paleoceanography*, **14**, 333-351, 1999.
- Patrick, A., and R. C. Thunell, Tropical Pacific sea surface temperatures and upper water column thermal structure during the Last Glacial Maximum, *Paleoceanography*, **12**, 649-657, 1997.
- Peixoto, J. P., and A. H. Oort, *Physics of Climate*, 520 pp. Am. Inst. of Physics, New York, 1992.
- Pickard, G. L., and W. J. Emery, *Descriptive Physical Oceanography: An Introduction*, 320 pp., Pergamon, New York, 1990.
- Pond, S., and G. L. Pickard (Eds.), *Introductory Dynamical Oceanography*, 329 pp., Pergamon, New York, 1983.
- Ravelo, A. C., and R. Fairbanks, Oxygen isotopic composition of multiple species of planktonic foraminifera: Recorders of modern photic zone temperature gradient, *Paleoceanography*, **7**, 815-831, 1992.
- Ravelo, A. C., and N. J. Shackleton, Evidence for surface water circulation changes at ODP Site 851 in the eastern tropical Pacific, *Proc. Ocean Drill. Program Sci. Results*, **138**, 503-514, 1995.
- Rodgers, K. B., M. A. Cane, N. H. Naik, and D. P. Schrag, The role of the Indonesian Throughflow in equatorial Pacific thermocline ventilation, *J. Geophys. Res.*, **104**, 20,551-20,570, 1999.
- Ruddiman, W. F., and A. McIntyre, Northeast Atlantic paleoclimatic changes over the last 600,000 years, *Geol. Soc. Am. Mem.*, **145**, 111-146, 1976.
- Schiffelbein, P., Extracting the benthic mixing impulse response function: A constrained deconvolution technique, *Mar. Geol.*, **64**, 313-336, 1985.
- Schmidt, G. A., Forward modeling of carbonate proxy data from planktonic foraminifera using oxygen isotope tracers in a global ocean model, *Paleoceanography*, **14**, 482-497, 1999.
- Schneider, R., P. J. Mueller, and G. Ruhland, Late Quaternary surface circulation in the east equatorial South Atlantic: Evidence from alkenone sea surface temperatures, *Paleoceanography*, **10**, 197-219, 1995.
- Schoenfeld, J., and H.-R. Kudrass, Hemipelagic sediment accumulation rates in the South China Sea related to quaternary sea-level changes, *Quat. Res.*, **40**, 368-379, 1993.
- Schrag, D. P., G. Hampt, and D. W. Murray, Pore fluid constraints on the temperature and oxygen isotopic composition of the glacial ocean, *Science*, **272**, 1930-1932, 1996.
- Sikes, E., and L. D. Keigwin, Equatorial Atlantic sea surface temperatures for the last 30 kyr: A comparison of  $U^{37}$   $\delta^{18}O$  and foraminiferal assemblage temperature estimates, *Paleoceanography*, **9**, 31-45, 1994.
- Shackleton, N. J., The oxygen isotope stratigraphic records of the Late Pleistocene, *Philos. Trans. R. Soc. London, Ser. B*, **280**, 169-182, 1977.
- Slowey, N. C., and W. B. Curry, Enhanced ventilation of the North Atlantic subtropical thermocline during the last glaciation, *Nature*, **358**, 665-668, 1992.
- Slowey, N. C., and W. B. Curry, Glacial-interglacial differences in circulation and carbon cycling within the upper western North Atlantic, *Paleoceanography*, **10**, 715-732, 1995.
- Spero, H. J. and M. J. DeNiro, The influence of symbiotic photosynthesis on the  $\delta^{18}O$  and  $\delta^{13}C$  values of planktonic foraminiferal shell calcite, *Symbiosis*, **4**, 213-228, 1987.
- Stott, L. D., and C. M. Tang, Reassessment of foraminiferal-based tropical sea surface  $\delta^{18}O$  paleotemperatures, *Paleoceanography*, **11**, 37-56, 1996.
- Thunell, R. C., Q. Miao, S. E. Calvert, and T. F. Pedersen, Glacial-Holocene biogenic sedimentation patterns in the South China Sea: Productivity variations and surface water  $pCO_2$ , *Paleoceanography*, **7**, 143-162, 1992.
- Thunell, R. C., D. Anderson, D. Gellar, and Q. Miao, Sea surface temperature estimates for the tropical western Pacific during the last glaciation and their implications for the Pacific warm pool, *Quat. Res.*, **41**, 255-265, 1994.
- Tsuchiya, M., R. Lukas, and R. A. Fine, Source waters of the Pacific Equatorial Undercurrent, *Prog. Oceanogr.*, **23**, 101-147, 1989.
- UNESCO, Background papers and supporting data on the international equations of state of seawater 1980, *UNESCO Tech. Pa. Sci.* **36**, 192 pp., 1981.
- Wang, L., and P. Wang, Late Quaternary paleoceanography of the South China Sea: glacial-interglacial contrast in an enclosed basin, *Paleoceanography*, **5**, 77-90, 1990.
- Wang, L., M. Sarnthein, J.-C. Duplessy, H. Erlenkeuser, S. Jung, and U. Pflaumann, Paleo sea surface salinities in the low-latitude Atlantic: The  $\delta^{18}O$  records of *Globigerinoides ruber* (white), *Paleoceanography*, **10**, 749-762, 1995.
- Wolff, T., S. Mulitza, H. Arz, J. Paetzold, G. Wefer, Oxygen Isotopes versus CLIMAP (18 ka) temperatures: A comparison from the tropical Atlantic, *Geology*, **26**, 675-678, 1998.
- Wyrtki, K., Oceanography of the eastern equatorial Pacific Ocean, *Oceanogr. Mar. Biol. Annu. Rev.*, **4**, 33-68, 1966.
- Zhang, R.-H., L. M. Rothstein, and A. J. Busalacchi, Origin of upper-ocean warming and El Niño change on decadal scales in the tropical Pacific Ocean, *Nature*, **391**, 879-883, 1998.

---

K. Billups and D. P. Schrag, Harvard University, Department of Earth and Planetary Sciences, 20 Oxford Street, Cambridge, MA 02138. (e-mail: billups@eps.harvard.edu).

(Received May 14, 1999;  
revised October 1, 1999;  
accepted October 7, 1999.)